ELSEVIER

Journal of Photochemistry and Photobiology A: Chemistry 144 (2001) 83–91

Journal of Photochemistry and Photobiology A:Chemistry

www.elsevier.com/locate/jphotochem

Optical properties of photochromic fluorinated indolylfulgides

Mason A. Wolak, Nathan B. Gillespie, Craig J. Thomas, Robert R. Birge, Watson J. Lees*

Department of Chemistry and W.M. Keck Center for Molecular Electronics, Syracuse University, Syracuse, NY 13244, USA

Received 4 June 2001; received in revised form 7 August 2001; accepted 9 August 2001

Abstract

Fluorinated indolylfulgides are a promising class of photochromic organic compounds for optical memory and switches. Absorption spectra, quantum yields, thermal stabilities, and photochemical fatigue resistances have been measured for a series of fluorinated indolylfulgides. The cyclizable form of the heptafluoropropyl-substituted 1,2-dimethylindolylfulgide displays the longest absorbance maxima yet reported for the cyclizable form of a fulgide. Photochemical durability was quantified in both solvent and polymer for the first time, with the trifluoromethyl derivative undergoing more than 2500 photochemical cycles before degrading by 20% in either environment. In addition, the thermal stability of the cyclizable form has been examined for the first time. Although each fulgide showed outstanding resistance to thermal stress in the *C*-form, the cyclizable form degraded rapidly at 80°C. These studies highlight the many advantageous properties associated with fluorination and identify areas for future improvements.

Keywords: Photochromism; Fulgide; Stability; Fluorination; 3D optical storage; Optical switches

1. Introduction

The phenomenon of photochromism is characterized by rapid, reversible transformations between different chemical states induced by absorption of light [1,2]. Reversible coloration and bleaching upon wavelength controlled illumination is an ideal characteristic for special inks and dyes, biological sensors, optical switches, and optical memory media [3]. Recently, research pertaining to photochromic organic compounds has focused upon development of material useful in a high capacity rewritable optical memory device. Material used in such a device must have readily distinguishable absorption spectra for each state, efficient photoreactions, and both thermal and photochemical stability.

Heterocyclic fulgides, a class of photochromic organic compounds, meet many of these requirements. In particular, indolyl substituted fulgides are noted for their high thermal stability and enhanced resistance to photochemical fatigue relative to other fulgides [4]. Additionally, the *E*-form of the methyl substituted indolylfulgide displays a bathochromic shift relative to other heteroaromatic fulgides and absorbs in the beginning of the visible region (Scheme 1) [5]. This feature is particularly attractive as absorption of light in the visible region allows the use of inexpensive light sources during the read/write cycle.

Despite extensive investigation of the spectral characteristics and photoreactions of a wide variety of fulgides, little has been published regarding the thermal and photochemical stability of these compounds [4,6,7]. Rewritable optical memory requires a highly robust compound that can easily withstand repeated coloration and bleaching along with elevated temperatures. Consequently, measurement of the material's ability to resist thermal stress and photochemical fatigue is of paramount importance.

To date, the most promising fulgide noted in the literature is trifluoromethyl substituted indolylfulgide **1**, originally reported by Yokoyama and Takahashi [8]. A notable attribute of the fluorinated indolylfulgide was the fact that its cyclizable *Z*-form showed the longest absorption maxima of any fulgide at 426 nm. It also featured increased quantum yields and was demonstrated to withstand 1000 repeated photochemical cycles in a poly(methylmethacrylate) (PMMA) polymer film without loss of absorbance. In addition, the *C*-form displayed remarkable thermal stability in PMMA film with no noticeable decomposition after being held at 80°C for 10 days.

Herein, we report the thermal and optical properties of a series of indolylfulgides substituted with perfluorinated alkyl chains of increasing length, beginning with Yokoyama's trifluoromethyl substituted indolylfulgide **1**. The compounds were prepared as previously reported [9] to investigate the

* Corresponding author. Tel.: +1-315-443-5803; fax: +1-315-443-4070.
E-mail address: wjlees@syr.edu (W.J. Lees).

1010-6030/01/$ – see front matter
PII: S1010-6030(01)00550-0

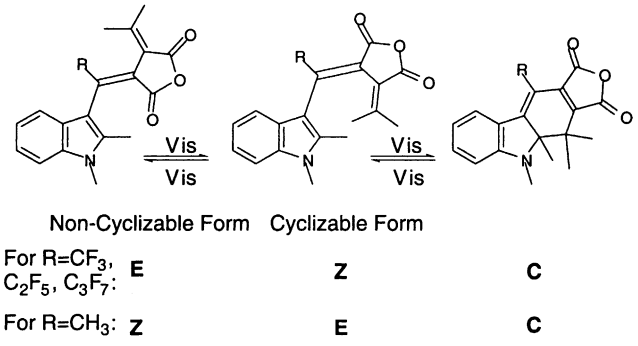

Scheme 1. Photochemical reactions of indolylfulgides **1**–**4**. R = CF_3 (**1**); R = C_2F_5 (**2**); R = n-C_3F_7 (**3**); R = CH_3 (**4**). For fluorinated indolylfulgides, the cyclizable form is the *Z*-form (due to IUPAC nomenclature). For virtually all other fulgides the *E*- and *Z*-forms are switched.

change in absorption spectra, quantum yields, and thermal and photochemical stability with perfluorinated alkyl chain length. Thermal stability for the cyclizable *Z*-form of each compound is reported for the first time. In addition, measurement of photochemical fatigue is presented for fluorinated indolylfulgides in both solution and polymer film.

2. Experimental details

2.1. Materials

2.1.1. Synthesis

Fulgides **1**–**3** were prepared in *Z*-isomer form as previously reported [9]. The *E*-isomers were prepared by irradiation of a solution of *Z*-isomer at 350 nm and purification by flash column chromatography (4:1 hexane:dioxane as eluent on silica gel) followed by crystallization from isopropanol. The *C*-isomers were obtained by irradiation of a solution of *Z*-isomer at 427 nm. The resulting crude product was then purified by flash column chromatography (toluene as eluent on silica gel) and used directly. Purity of each compound was verified by a Hitachi D-7000 HPLC using a Waters Spherisorb S5 W column with 85:15 hexane:dioxane as the eluent at a flow rate of 2.5 ml/min. All ^{1}H NMR spectra were acquired on a Bruker 300 MHz NMR spectrometer and internally referenced to $CHCl_3$ at 7.26 ppm or acetone at 2.05 ppm. (**1**) *C*-form: ^{1}H NMR ($CDCl_3$) δ 7.76 (d, J = 8.3 Hz, 1H), 7.41 (td, J = 8.3, 1.2 Hz, 1H), 6.81 (td, J = 8.3, 1.2 Hz, 1H), 6.67 (d, J = 8.3 Hz, 1H), 2.96 (s, 3H), 1.78 (s, 3H), 1.37 (s, 3H), 1.24 (s, 3H); *E*-form: ^{1}H NMR ($CDCl_3$) δ 7.46–7.10 (m, 4H), 3.75 (s, 3H), 2.49 (s, 3H), 2.37 (s, 3H), 2.28 (q, J = 2.8 Hz, 3H); *Z*-form: ^{1}H NMR ($CDCl_3$) δ 7.37–7.11 (m, 4H), 3.71 (s, 3H), 2.28 (s, 3H), 2.16 (s, 3H), 0.97 (s, 3H), Anal. Calcd. for $C_{19}H_{16}F_3NO_3$: C, 62.81; H, 4.44; F, 15.69; N, 3.86. Found: C, 62.58; H, 4.06; F, 15.52; N, 3.77. (**2**) *C*-form: ^{1}H NMR (CD_3COCD_3) δ 7.74 (d, J = 8.1 Hz, 1H), 7.47 (td, J = 8.1, 1.2 Hz, 1H), 6.89 (d, J = 8.1 Hz, 1H), 6.82 (td, J = 8.1, 1.2 Hz, 1H), 3.10 (s, 3H), 1.84 (s, 3H), 1.52 (s, 3H), 1.22 (s, 3H); *E*-form (from mixture of *E*- and *Z*-form): ^{1}H NMR ($CDCl_3$) δ 7.45–7.16 (m, 4H), 3.74 (s, 3H), 2.48 (s, 3H), 2.32 (s, 3H), 2.27 (t, J = 2.8 Hz, 3H); *Z*-form: ^{1}H NMR ($CDCl_3$) δ 7.35–7.12 (m, 4H), 3.69 (s, 3H), 2.24 (s, 3H), 2.12 (s, 3H), 1.09 (s, 3H), Anal. Calcd. for $C_{20}H_{16}F_5NO_3$: C, 58.12; H, 3.90; F, 22.98; N, 3.39. Found: C, 58.09; H, 3.60; F, 23.11; N, 3.31. (**3**) *C*-form: ^{1}H NMR ($CDCl_3$) δ 7.74 (d, J = 8.4 Hz, 1H), 7.40 (td, J = 7.8, 1.1 Hz, 1H), 6.78 (td, J = 7.8, 1.2 Hz, 1H), 6.67 (d, J = 8.4 Hz, 1H), 3.00 (s, 3H), 1.79 (s, 3H), 1.42 (s, 3H), 1.22 (s, 3H); *E*-form: ^{1}H NMR ($CDCl_3$) δ 7.45 (d, J = 7.8 Hz, 1H), 7.31 (d, J = 8.0 Hz, 1H), 7.22 (td, J = 7.5, 1.1 Hz, 1H), 7.13 (td, J = 7.9, 1.1 Hz, 1H), 3.74 (s, 3H), 2.47 (s, 3H), 2.35 (s, 3H), 2.28 (t, J = 2.8 Hz, 3H); *Z*-form: ^{1}H NMR ($CDCl_3$) δ 7.35 (d, J_{HH} = 7.7 Hz, 1H), 7.29 (d, J_{HH} = 8.0 Hz, 1H), 7.25 (td, J_{HH} = 7.8 Hz, J_{HH} = 0.9 Hz, 1H), 7.12 (dt, J_{HH} = 7.8 Hz, J_{HH} = 0.9 Hz, 1H), 3.69 (s, 3H), 2.25 (s, 3H), 2.13 (s, 3H), 1.09 (s, 3H), Anal. Calcd. for $C_{21}H_{16}F_7NO_3$: C, 54.44; H, 3.48; F, 28.70; N, 3.02. Found: C, 54.36; H, 3.22; F, 28.65; N, 2.98.

Fulgide **4** was prepared as the *E*-isomer according to the literature [10]. The *E*-isomer was purified by flash column chromatography (CH_2Cl_2 as eluent on silica gel) and crystallized from isopropanol. The *C*-isomer was obtained by irradiation of a solution of *E*-isomer at 416 nm. The crude product was then purified by column chromatography (CH_2Cl_2 as eluent on silica gel) and used directly. Purity of each isomer was verified via HPLC in a similar manner as stated above.

2.1.2. Thin films

Thin films were prepared by adding 2–4 mg of the cyclizable form or the *C*-form of the fulgide to a 5 ml solution of 10% PMMA (low molecular weight, Aldrich) in CH_2Cl_2, followed by solution deposition on 1 in. × $\frac{1}{16}$ in. BK-7 glass slides (escoproducts). The polymer solution was allowed to dry overnight at room temperature. The resulting films varied in thickness from 100 to 200 μm and were utilized in both thermal and photochemical stability studies.

2.2. Spectroscopic measurements

Concentrated, air-saturated stock solutions of both the *Z*- and *E*-isomer of fulgides **1**–**3** in toluene were prepared in duplicate or triplicate. From each stock solution, four or five samples ranging in concentration from 0.20 to 0.05 mM were then prepared by dilution with toluene. Absorption coefficients and λ_{max} were determined using a Cary 1 spectrophotometer. The freshly purified *C*-isomers were diluted four or five times and spectra were obtained in an identical manner. Each *C*-isomer solution was quantitatively converted to *Z*-isomer with 580 nm light and the concentration of fulgide present was ascertained using the predetermined *Z*-isomer extinction coefficients. Absorption coefficients and λ_{max} for the *C*-isomers were then determined from the initial spectra.

2.3. Irradiation

2.3.1. Quantum yields

Quantum yields for ring-closing (Φ_{ZC}) and *E* to *Z* photoisomerization reactions (Φ_{EZ}) were determined with monochromatic light of wavelength 427 nm. Quantum yields for ring-opening reactions (Φ_{CZ}) were determined with monochromatic light of wavelength 559 nm. A Coherent Infinity XPO laser system served as the irradiation source for all quantum yield experiments. Air-saturated solutions of all three isomers of fulgides **1**–**3** were prepared in toluene. The concentration of each solution was approximately 0.1 mM. Samples were irradiated to between 5 and 10% conversion as determined by HPLC and UV–Vis. Coherent LMP-2 energy detectors measured the amount of light absorbed by the fulgide solution in comparison to a toluene blank. Separation of isomers for the coloration and bleaching reactions was achieved on a Hitachi D-7000 HPLC using a Waters Spherisorb S5 W column with toluene as the eluent at a flow rate of 4.0 ml/min. Separation of isomers for the *E* to *Z* photoisomerization reaction was achieved using the same column with 85:15 hexane:dioxane as the eluent at a flow rate of 2.7 ml/min. The apparatus was calibrated with the chemical actinometer trioxalatoferrate(III) [11] and Aberchrome 540, a furylfulgide [12]. Quantum yields for *Z* to *E* photoisomerization (Φ_{ZE}) were determined via photostationary state (PSS) measurement as detailed below.

2.3.2. PSS measurements

Fulgides **1**–**3** were irradiated with 427 nm light supplied by a Coherent Infinity XPO laser and their isomeric ratios monitored via HPLC until a PSS ($PSS_{427\,nm}$) was attained. The isomers were separated on a Hitachi D-7000 HPLC using a Waters Spherisorb S5 W column with 85:15 hexane:dioxane as the eluent at a flow rate of 2.7 ml/min. A 1:1:1 mixture of the three isomers in toluene was analyzed via HPLC to ascertain their relative extinction coefficients in the HPLC solvent. Quantum yields for Φ_{ZE} and Φ_{CZ} at 427 nm were determined from the PSS measurements.

2.3.3. Photochemical fatigue

2.3.3.1. Solution-based study. Air-saturated solutions of the *Z*-isomer of fulgides **1**–**3** were prepared in toluene with an initial absorbance of 0.600 at the visible absorption maxima. An air-saturated solution of the *E*-isomer of fulgide **4** was prepared in toluene with an initial absorbance of 1.800 at the absorption maximum (due to the material's minimal absorption coefficient at 436 nm). Samples were irradiated to PSS with light supplied from an Oriel 1000 W QTH lamp utilizing a 436 nm narrow bandpass filter. After measuring the UV–Vis spectra of the $PSS_{436\,nm}$ mixture, solutions were irradiated to 90% of the PSS and the reaction was timed. The 90% PSS mixture was then bleached with >530 nm light using a separate filter. Absorbance at the *C*-isomer λ_{max} was <0.01 upon bleaching.

Once the duration of irradiation was established for both the 90% PSS coloration and <1% *C*-isomer bleaching reactions, the system was automated through the use of a filter wheel. All solutions were capped and stirred. Control experiments were performed to correct for evaporation. After a designated number of irradiation cycles, the samples were fully converted to $PSS_{436\,nm}$ and their UV–Vis spectra were scanned. The photochemical fatigue was then determined by comparison with the initial $PSS_{436\,nm}$ absorption spectra. The percentage of degradation per photochemical cycle was determined by fitting the experimental data to a exponential decay function.

2.3.3.2. Polymer-based study. PMMA films containing the *Z*-isomer of fulgides **1**–**3** were converted to predominantly *C*-isomer by irradiation to $PSS_{430\,nm}$ with light supplied by a Coherent Infinity XPO system. PMMA films for fulgide **4** were prepared with freshly purified *C*-isomer. The visible spectrum of each film was obtained with a Hewlett-Packard 8453 spectrophotometer before being placed in a thermally controlled ($20 \pm 1^{\circ}C$) holder. To ascertain the initial rate of *C* to *Z* conversion, a photokinetic trace was obtained using 501.7 nm (fulgides **1**–**3**) or 457.8 nm (fulgide **4**) light from a Coherent Innova 308C argon-ion laser (Ar-ion). The change in transmitted power was measured with a Coherent LM-2 energy meter and a Coherent Ultima data acquisition unit interfaced to a PC via RS-232 protocol. Irradiation wavelengths were selected so as to provide appreciable amounts of both the *C*-isomer and the cyclizable isomer at PSS. Upon completion of the photokinetic trace, the entire film was then converted to PSS at the appropriate wavelength with the Ar-ion laser and another visible spectrum acquired. To determine photochemical fatigue, the films were subsequently irradiated with the Ar-ion laser at the appropriate wavelength for several hours at constant power (50–200 mW/cm^2, ±1% stability). Degradation of fulgides **1**–**3** was followed by monitoring the transmitted power as before. Films of fulgide **4** were monitored with a polarized 5 mW, 632.8 nm helium–neon laser (Melles Griot 05LHP151) at a low incident angle. The average transmitted power through a PMMA film without fulgide was used as a blank. From these results the photochemical fatigue was calculated (see Appendix A).

2.4. Thermal stability

Thin films containing either *Z*- or *C*-isomer of fulgides **1–3** were wrapped in aluminum foil and placed in an oven maintained at 80°C. The films were removed at prescribed intervals and their UV–Vis spectra were scanned on a Hewlett-Packard 8453 spectrophotometer. The films were monitored for the shorter of 10 days or until no further changes occurred in the UV–Vis spectra.

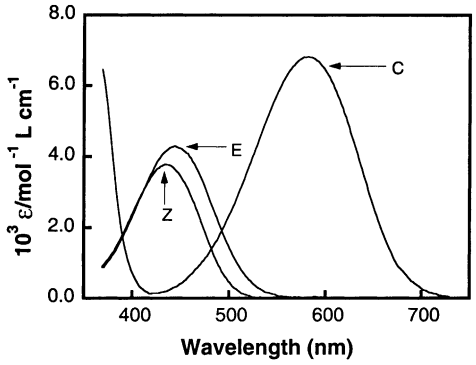

Fig. 1. UV–Vis absorption spectra of fulgide **3** in toluene.

Table 1
Extinction coefficients at λ_{max} for fulgides **1**–**4** in toluene

Fulgide	λ_{max}/nm (ε_{max}/mol^{-1} l cm^{-1})		
	Cyclizable form[a]	Non-cyclizable form	*C*-form
1	427 (5300)	441 (5600)	571 (6400)
2	432 (4400)	441 (4400)	580 (7100)
3	434 (3800)	444 (4300)	582 (6300)
4	385 (6810)	397 (14 300)	584 (7080)

[a] For fluorinated indolylfulgides **1**–**3**, the cyclizable form is the *Z*-form and the non-cyclizable form is the *E*-form, as per IUPAC nomenclature rules. For non-fluorinated analog **4** [5], the cyclizable form is the *E*-form and the non-cyclizable form is the *Z*-form.

3. Results and discussion

3.1. UV–visible absorption spectra

Fig. 1 displays the UV–visible absorption spectra of the *Z*-, *E*-, and *C*-forms of fulgide **3** measured in toluene. The wavelength of maximum absorbance and the corresponding extinction coefficients of **1**–**3** in toluene are presented in Table 1. A slight bathochromic shift is evident as the length of the perfluorinated alkyl chain increases; fulgide **3** has the longest *Z*-form absorption maxima yet reported. Although lengthening the perfluorinated alkyl chain had little effect on the extinction coefficients of the *C*-forms, lowered values were observed for the *Z*- and *E*-forms of **2** and **3**.

3.2. Quantum yields

The photochemical efficiencies for the various photoreactions presented in Scheme 1 were probed at different wavelengths corresponding to the reaction type. The quantum yield of the ring-closure reaction, Φ_{ZC}, for fulgides **1**–**3** was measured in toluene with 427 nm light. Measurement of Φ_{EZ} and Φ_{ZE} was also accomplished at the same wavelength, which was chosen to match the absorption maxima of fulgide **1**. Utilization of 427 nm light allows for a high percentage conversion of *Z*-form to *C*-form before the back reaction (ring-opening) becomes an issue, thereby improving the accuracy of quantum yield measurement. In addition, use of 427 nm light minimizes the *E*-form contribution, allowing for easier data analysis. As a consequence of these two factors, $PSS_{427\,nm}$ for fulgide **1** contains 95% *C*-form. In comparison, $PSS_{403\,nm}$ for fulgide **1** contains only 33% *C*-form [8]. For the ring-opening reaction (Φ_{CZ}), 559 nm light was chosen, matching the wavelength used in Yokoyama's work [8]. Quantum yield data is summarized in Table 2.

Fluorinated fulgides display an enhanced coloration quantum yield ($\Phi_{ZC} = 0.15$–0.20) relative to non-fluorinated analog **4** ($\Phi_{EC} = 0.040$ at 403 nm) [5]. According to the molecular modeling calculations (MNDOCI) comparing fulgides **1** and **4**, this can be attributed to a shift in the dipole for the indole moiety, generating more favorable π-overlap on the bond forming carbons of the cyclizable isomer. Previous work on indolylfulgides suggested that an increase in the steric bulk on the bridging alkene should augment the quantum yield of the ring-closing reaction [13,14]. It was expected that increasing the size of the perfluorinated chain would achieve the same outcome. Unfortunately, electronic effects seem to counterbalance steric effects as fulgides **2** and **3** gave mixed results.

Quantum yields for the bleaching reaction ($\Phi_{CZ} = 0.034$–0.043 at 559 nm) are relatively constant throughout the series and represent a modest decrease relative to non-fluorinated analog **4** ($\Phi_{CE} = 0.051$ at 559 nm). Steric considerations are significant with regards to *Z* and *E* photoisomerization. Fulgides **2** and **3** show a marked decrease in Φ_{ZE} and Φ_{EZ} relative to fulgide **1**. Despite the lowered efficiency of *Z*- to *E*-isomerization, there remains a small, but quantifiable concentration of *E*-form in the PSS at 427 nm. Modification of the excitation wavelength used to initiate ring-closure may result in further minimization of *E*-form concentration.

The PSS attained upon irradiation at 427 nm yields near quantitative conversion to *C*-form for **1**–**3**. Because the *C*-form maintains a modest absorption in this region ($\varepsilon_{427\,nm} < 400$ mol^{-1} l cm^{-1}) there is enough ring-opening to prevent ever attaining 100% conversion to *C*-form.

Table 2
Quantum yields of photoreactions for fulgides **1**–**3** in toluene

Fulgide	Irradiation at 427 nm				Irradiation at 559 nm, Φ_{CZ}	*C*:*Z*:*E* at $PSS_{427\,nm}$
	Φ_{ZC}	Φ_{CZ}	Φ_{ZE}	Φ_{EZ}		
1	0.20	0.10	0.014	0.022	0.043	95:3:2
2	0.15	0.15	0.003	0.010	0.034	93:5:2
3	0.18	0.16	0.002	0.007	0.042	95:4:1

Table 3
Thermal resistivity of fulgides **1**–**3** at 80°C in PMMA film

Fulgide	Thermal decomposition[a]		
	Z–A/A_0 (17.5 h)	C–A/A_0 (17.5 h)	C–A/A_0 (85 h)
1	0.75	0.94	0.90
2	0.56	0.96	0.94
3	0.55	0.98	0.98

[a] A/A_0 refers to the absorbance relative to the initial value at the maximum wavelength for the indicated isomer at 80°C after the denoted time.

Although complete conversion to *C*-form is never achieved for **1**–**3**, it is important to note that the non-fluorinated analog **4** exhibits only 56% conversion to *C*-form upon PSS irradiation at 405 nm [8]. Differentiation of the *Z*- and *C*-form absorption spectra for the fluorinated fulgides accounts for outstanding control of the coloration and bleaching photoreactions.

3.3. Thermal stability

One of the most important characteristics of a material to be used as optical memory is thermal stability at both ambient and elevated temperatures. Thermal stability was investigated for both the *Z*- and *C*-forms in the polymer PMMA. Fulgides **1**–**4** proved extremely stable at room temperature; no change in absorption spectra for either form was evident after 1 month. However, at 80°C, the *Z*-forms of **1**–**3** experienced relatively rapid decomposition. After 17.5 h, the absorbance of fulgide **3***Z* at 435 nm decreased by 45% (Table 3). Inspection of time dependent UV–Vis absorption spectra of **1***Z* reveals an initial decrease in absorbance followed by a red shift to a λ_{max} of 475 nm and subsequent increase in absorbance (Fig. 2). Lack of an isosbestic point suggests an intermediate is generated before the final degradation product is obtained. Examination of solution-based thermal degradation is currently underway [15].

The *C*-forms demonstrated significantly improved thermal stability at 80°C relative to the corresponding *Z*-forms. The absorbance of fulgide **2***C* at 580 nm decreased by only 6% after 85 h (Fig. 3). Little difference is seen between fulgides **1**–**3**. Ultimately, the thermal stability of an optical memory will be limited by the least stable memory element; for fluorinated indolylfulgides this corresponds to the *Z*-form.

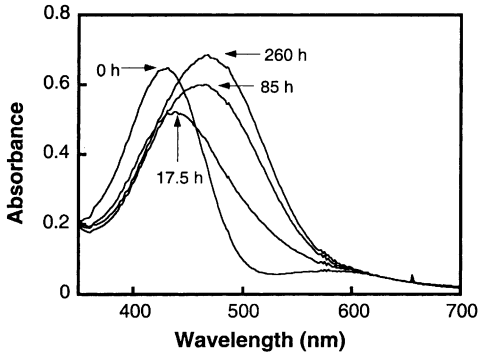

Fig. 2. UV–Vis absorption spectra of **1***Z* in PMMA with continuing treatment at 80°C.

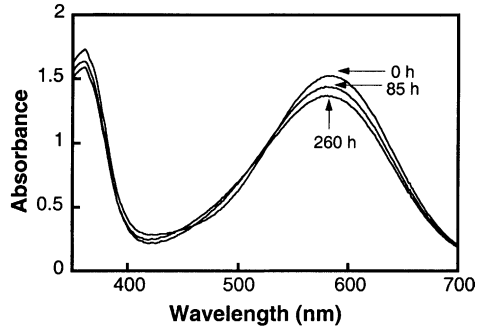

Fig. 3. UV–Vis absorption spectra of **2***C* in PMMA with continuing treatment at 80°C.

3.4. Photochemical stability

Kaneko et al. [4] have determined that non-fluorinated indolylfulgide **4** in PMMA degrades at a rate of 0.1% per photochemical cycle; coloration followed by bleaching. Rentzepis and co-workers [7] has illustrated similar fatigue resistance for 2-indolylfulgides in solution. Oxazolyl fulgides have also exhibited impressive photochemical stability, degrading at a rate of <0.03% per cycle [16]. In each of the aforementioned experiments, separate illumination was provided to initiate the ring-closing and ring-opening reactions.

The photochemical fatigue resistance of fulgides **1**–**4** in both toluene solution and PMMA is illustrated in Table 4. In solution, fluorinated indolylfulgides **1**–**3** display enhanced

Table 4
Photochemical fatigue resistance of fulgides **1**–**4**

Fulgide	Photochemical decomposition					
	In toluene			In PMMA		
	Number of cycles	A/A_0	%/cycle	Number of cycles	A/A_0	%/cycle
1	3000	0.791	0.007	4000	0.800	0.005
2	750	0.802	0.030	280	0.800	0.08
3	2250	0.784	0.011	220	0.800	0.09
4	300	0.875	0.057	425	0.800	0.05

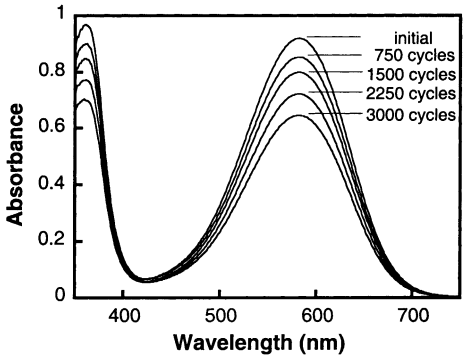

Fig. 4. PSS absorbances of fulgide **3** in toluene after the indicated number of cycles.

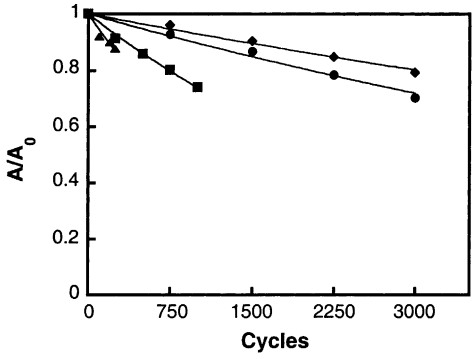

Fig. 5. Photochemical decomposition of **1**–**4** in toluene; decreasing absorbance with repeated coloration and bleaching cycles: diamonds (**1**), squares (**2**), circles (**3**) and triangles (**4**).

photochemical fatigue resistance relative to non-fluorinated indolylfulgide **4**. Although compound **1** is the most stable, heptafluoropropyl-indolylfulgide **3** can also withstand over 2000 photochemical cycles before degrading by 20% (Figs. 4 and 5). Fulgide **2** is roughly one-third as stable as **3**; rapidly losing 20% of its absorbance after only 750 cycles. The extremely slow degradation of **1** and **3** in solution represents the first fulgides to have comparable photochemical stability to diarylethenes [17].

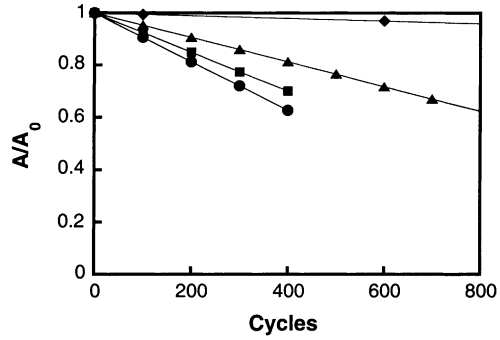

Fig. 6. Photochemical decomposition of **1**–**4** in PMMA; decreasing absorbance with repeated coloration and bleaching cycles: diamonds (**1**), squares (**2**), circles (**3**) and triangles (**4**).

Investigation of photochemical stability in PMMA films was accomplished by continuous irradiation with a single wavelength of light (Fig. 6). The wavelength was chosen such that an appreciable amount of both the cyclizable isomer and *C*-form were present at PSS (**1**–**3**, 501.7 nm; **4**, 457.8 nm). Data collected for fulgides **1** and **4** proved to be comparable to the solution study, but compounds **2** and **3** were not comparable. The difference in results between solution and polymer may be reasonable given that optical properties such as absorptivity, quantum yield, and wavelength are environment-dependent [7].

Yokoyama has suggested that photochemical decomposition of **4** can be attributed in part to hydrogen migration via 1,5-sigmatropic rearrangement (Scheme 2) [8]. Subsequent tautomerization of the resulting compound would re-establish the anhydride and thereby destroy conjugation between the indole and cyclic anhydride moieties. The new material would undergo a blue shift and no longer be photochromic in nature. Based upon this hypothesis, Yokoyama synthesized **1**, thus eliminating the possibility of a hydrogen shift from the methyl group as a fluorine atom is not likely to undergo a similar migration. Indeed, fulgide **1** shows enhanced photochemical fatigue resistance in both solution and polymer relative to fulgide **4**. Fulgides **2** and **3** also cannot undergo a 1,5-hydrogen shift from the methyl group and

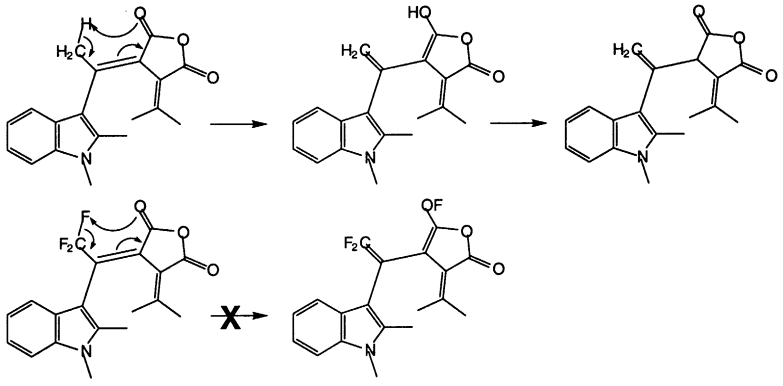

Scheme 2. Potential photochemical degradation pathway for **1** and **4**.

thus might be expected to have similar photochemical stability to **1**. Similar stability is observed in solution, but not in polymer films. The degradation pathways for **1**–**3** are at present unclear; photodegradation products in solution have not been detected by HPLC using the standard solvent systems for fulgides. Unfortunately, few examples of the isolation and characterization of photodegradation products for photochromic materials exist in the literature [18].

4. Conclusion

Fluorinated indolylfulgides have many propitious properties relative to their non-fluorinated analogs, making them suitable for inclusion in optical memory devices. The advantages of fluorination include longer wavelength λ_{max} for the cyclizable isomer, near quantitative conversion to *C*-form at $PSS_{427\,nm}$, and enhanced photochemical stability and coloration quantum yields. Fulgide **3** has the longest wavelength λ_{max} for the cyclizable isomer yet reported for a fulgide. At PSS irradiation with 427 nm light, all three fluorinated compounds contain >93% *C*-form. All three fulgides in solution degrade at a rate slower than any other fulgide previously reported. Unexpectedly, fulgides **1**–**3** have similar coloration quantum yields unlike their non-fluorinated analogs, suggesting electron withdrawing ability is more important than steric effects. Furthermore, we have provided for the first time quantitative data for the percent degradation per photochemical cycle and *Z*-form thermal stability of fluorinated indolylfulgides. Areas for further improvement have been identified and will be explored in the expectation of preparing improved photochromic materials.

Acknowledgements

Financial support from the National Science Foundation (NSF CHE9975076 to W.J.L.), the Army Research Office (MURI program, DAAD19-99-1-0198 to R.R.B.), and the National Institutes of Health (GM-34548 to R.R.B.) is gratefully acknowledged.

Appendix A. Measurement of fulgide photochemical durability in PMMA films at PSS

We introduce here the theoretical basis for our method of measuring the photochemical durability of the fulgides synthesized in this investigation in PMMA thin films. Our approach is based on the use of continuous illumination of a PSS, and has the advantage of providing a rigorous and reproducible experimental value. It has the disadvantage of limiting the wavelengths that can be used to measure the cyclicity because only those wavelengths of light that are absorbed by both the initial and final photochemical states can be used. This limitation is a minor inconvenience if one has access to the necessary laser systems. In our approach, we also take advantage of the spectral isolation of the *C*-form to obtain its rate of conversion to the cyclizable form at a PSS. From this rate, one can obtain the number of times that all of the remaining photochromic molecules in the sample have been converted from the colored form to the cyclizable form and back again. The basic photochemical pathway observed in the fluorinated indolylfulgides is illustrated in Scheme 3.

We include the possibility of degradation pathways from all three species, although we have not verified that all three pathways are relevant to the molecules under study. We note that the IUPAC convention for labeling these molecules can lead to confusion. The *Z* label is given when the highest priority (highest atomic number) groups are in a *cis* conformation across the adjacent double bond. *E* is assigned for a *trans* conformation. R1 has the highest priority in flourinated indolylfulgides, and the lowest for most others. Hence, the cyclizable form is given the *Z* label when R1 is a flourinated group, and an *E* label when it is an alkyl group. In this appendix, we label *Z* as the cyclizable form, because flourinated indolylfulgides are the focus of this paper.

The following assumptions are made to derive our model for measuring the cyclicity. First, none of the degradation products absorb at the actinic or probe wavelengths. Second, the overall rate of conversion from *C*- to *Z*-form (cyclizable) dominates when $[C] \gg [Z]$. Third, the time required to reach a PSS is much shorter than the time required to achieve significant photochemical degradation. From these

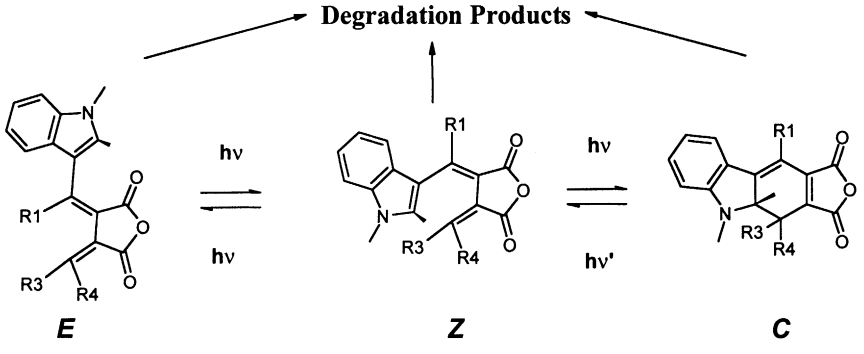

Scheme 3.

assumptions, the following equation can be derived for the *C*-form [19]:

$$\frac{d[C]}{dt} = (\varepsilon_Z[Z]\phi_{ZC} - \varepsilon_C[C]\phi_{CZ})\frac{I_0(1-10^{-A})}{A} \quad (A.1)$$

where A is the sample absorbance at the actinic wavelength, t the time, $[C]$ the concentration of *C*-isomer, $[Z]$ the concentration of *Z*-isomer, ε_Z the extinction coefficient of *Z*, ε_C the extinction coefficient of *C*, ϕ_{ZC} the quantum yield of *Z* to *C* photochemistry and ϕ_{CZ} the quantum yield of the reverse reaction (*C* to *Z*).

Assuming $[C] \gg [Z]$, one obtains:

$$\frac{d[C]}{dt} = \varepsilon_C[C]\phi_{CZ}\frac{I_0(1-10^{-A})}{A} \quad (A.2)$$

Applying the Beer–Lambert law to Eq. (A.2) results in the following equation:

$$\frac{dA_C}{dt} = -\varepsilon_C\phi_{CZ}I_0\frac{(1-10^{-A})}{A} \quad (A.3)$$

Here A_C is the absorbance of *C*-form at the actinic wavelength. When the fraction of *C*-form is high then $A_C \sim A$ and the equation can be simplified to

$$\frac{dA_C}{dt} = -\varepsilon_C\phi_{CZ}I_0(1-10^{-A}) \quad (A.4)$$

In addition when the fraction of *C*-form is high, the change in absorbance upon illumination at the actinic wavelength corresponds almost exclusively to the conversion of *C*-form to *Z*-form. Since for every molecule of *C*-form lost one of *Z*-form is generated, Eq. (A.2) can be rearranged to

$$\frac{d[C]}{dt} = -\frac{d[Z]}{dt} = -\varepsilon_C[C]\phi_{CZ}\frac{I_0(1-10^{-A})}{A} \quad (A.5)$$

Applying the Beer–Lambert law to Eq. (A.5) and assuming $A_C \sim A$, one obtains

$$\frac{dA_Z}{dt} = \varepsilon_Z\phi_{CZ}I_0(1-10^{-A}) \quad (A.6)$$

Here A_Z is the absorbance of *Z*-form at the actinic wavelength. The change in overall absorbance A with time at the actinic wavelength when the fraction of *C*-form is high then becomes

$$\frac{dA}{dt} = \frac{dA_C}{dt} + \frac{dA_Z}{dt} = (\varepsilon_Z - \varepsilon_C)\phi_{CZ}I_0(1-10^{-A}) \quad (A.7)$$

Separation and integration of both sides of Eq. (A.7) yields:

$$\int_{A_0}^{A} \frac{dA}{I_0(1-10^{-A})}(\varepsilon_Z - \varepsilon_C)\phi_{CZ}t \quad (A.8)$$

where A_0 the initial absorbance at the actinic wavelength. From the early traces (<10% conversion) of a photokinetic analysis for each thin film, we can derive a constant, $\mathbf{k} = (\varepsilon_C - \varepsilon_Z)\phi_{CZ}$ by numerically integrating the left-hand side of this equation with respect to A, and plotting its value with respect to time. The constant $\mathbf{k}_{CZ}$ which corresponds to $\varepsilon_C\phi_{CZ}$, can then be determined from the ratio of extinction coefficients of *C* and *Z* at the actinic wavelength, $r = \varepsilon_C/\varepsilon_Z$; $\mathbf{k}_{CZ} = \varepsilon_C\phi_{CZ} = \mathbf{k}r/(r-1)$. At the PSS, in terms of *C*-form absorbance at the actinic wavelength, the rates of *C* to *Z*, $(dA_C/dt)_{CZ}$, and *Z* to *C*, $(dA_C/dt)_{ZC}$, interconversion are equal:

$$\frac{dA_C}{dt} = \left(\frac{dA_C}{dt}\right)_{ZC} + \left(\frac{dA_C}{dt}\right)_{CZ} = 0 \quad (A.9)$$

Hence, we can obtain the rate of *C* to *Z* interconversion in absorbance per unit time, via the substitution of $\mathbf{k}_{CZ}$ into Eq. (A.3), assuming all of the other parameters were obtained from the experiment. This results in the following relationship for PSS, wherein A_C can be extrapolated from spectra

$$\left(\frac{dA_C}{dt}\right)_{CZ} = -k_{CZ}A_C I_0\frac{(1-10^{-A})}{A} \quad (A.10)$$

A photochromic cycle is then defined as the complete conversion of all of the molecules in the film from *Z*- to *C*-form and back again. The number of photochromic cycles (ΔN) in a given time interval (Δt) can be obtained from the following equation:

$$\Delta N = \frac{(dA_C/dt)_{CZ}}{(A_{pss}/A_{pss_0})A_{C_0}}\Delta t \quad (A.11)$$

Summation of the number of cycles at each time interval renders the total average number of cycles that have occurred in the irradiated volume. The initial factor (A_{pss}/A_{pss_0}, where A_{pss} is the photostationary state absorbance at time t, and A_{pss_0} is the initial value of A_{pss}) corrects for the loss of photochromic molecules as the film degrades. Hence, the number of molecules participating in a cycle increases as a function of time. The asymptote representing the 50% degradation point is estimated by using straight line extrapolation. All the data collected are consistent with this approach and the corollary assumption of a first-order decay process with an unknown number of decay paths.

References

[1] J.C. Crano, R.J. Guglielmetti (Eds.), Organic Photochromic and Thermochromic Compounds, Vol. 1, Plenum Press, New York, 1999.
[2] H. Durr, H. Bousas-Laurent, Photochromism, Molecules and Systems, Elsevier, Amsterdam, 1990.
[3] Y. Yokoyama, Chem. Rev. 100 (2000) 1717.
[4] A. Kaneko, A. Tomoda, M. Ishizuka, H. Suzuki, R. Matsushima, Bull. Chem. Soc. Jpn. 61 (1988) 3569.
[5] Y. Yokoyama, T. Tanaka, T. Yamane, Y. Kurita, Chem. Lett. (1991) 1125.
[6] R. Matsushima, H. Sakaguchi, J. Photochem. Photobiol. A 108 (1997) 239.
[7] Y.C. Liang, A.S. Dvornikov, P.M. Rentzepis, J. Photochem. Photobiol. A 125 (1999) 79.

[8] Y. Yokoyama, K. Takahashi, Chem. Lett. (1996) 1037.
[9] C.J. Thomas, M.A. Wolak, R.R. Birge, W.J. Lees, J. Org. Chem. 66 (2001) 1914.
[10] S.Z. Janicki, G.B. Schuster, J. Am. Chem. Soc. 117 (1995) 8524.
[11] N.J. Bunce, Actinometry, in: J.C. Scaiano (Ed.), Handbook of Organic Photochemistry, Vol. 1, CRC Press, Boca Raton, 1989, 241 pp.
[12] H.G. Heller, Spec. Publ. R. Soc. Chem. 60 (1986) 120.
[13] Y. Yokoyama, T. Goto, T. Inoue, M. Yokoyama, Y. Kurita, Chem. Lett. (1988) 1049.
[14] Y. Yokoyama, T. Inoue, M. Yokoyama, T. Goto, T. Iwai, N. Kera, I. Hitomi, Y. Kurita, Bull. Chem. Soc. Jpn. 67 (1994) 3297.
[15] M.A. Wolak, J.M. Sullivan, C.J. Thomas, R.C. Finn, R.R. Birge, W.J. Lees, J. Org. Chem. 66 (2001) 4739.
[16] H. Suzuki, A. Tomoda, M. Ishizuka, A. Kaneko, M. Furui, R. Matsushima, Bull. Chem. Soc. Jpn. 62 (1989) 3968.
[17] M. Irie, K. Uchida, Bull. Chem. Soc. Jpn. 71 (1998) 985.
[18] M. Irie, T. Lifka, K. Uchida, S. Kobatake, Y. Shindo, Chem. Commun. (1999) 747.
[19] E. Uhlmann, G. Gauglitz, J. Photochem. Photobiol. A 98 (1996) 45.